dos Reis, M., P.M.L.A. Graça, A.M. Yanai, C.J.P. Ramos & P.M. Fearnside. 2021. **Forest fires and deforestation in the central Amazon: Effects of landscape and climate on spatial and temporal dynamics**. *Journal of Environmental Management* 88: art. 112310. https://doi.org/10.1016/j.jenvman.2021.112310

DOI: 10.1016/j.jenvman.2021.112310
ISSN: 0301-4797

Title: Forest Fires and Deforestation in the Central Amazon: Effects of Landscape and Climate on Spatial and Temporal Dynamics

Abstract

Forest fires and deforestation are the main threats to the Amazon forest. Extreme drought events exacerbate the impact of forest fire in the Amazon, and these drought events are predicted to become more frequent due to climate change. Fire escapes into the forest from agriculture and pasture areas. We assessed the potential drivers of deforestation and forest fires in the central Brazilian Amazon and show that over a period of 31 years (1985 to 2015) forest fires occurred only in years of extreme drought induced by El Niño (1997, 2009 and 2015). The association of forest fires with strong El Niños shows the vulnerability of forest to climate change. The areas deforested were closely associated with navigable rivers: 62% of the total deforestation from 2000 to 2018 was located within the 2 km of rivers. There was a notable increase in deforestation and forest fire during the 2015 El Niño in comparison to previous years. Only a small part of the forest that burned was deforested in the years following the wildfires: 7% (1997), 3% (2009) and 1.5% (2015). Forest close to roads, rivers and established deforestation is susceptible to deforestation and fire since these areas are attractive for agriculture and pasture. Indigenous land was shown to be important in protecting the forest, while rural settlement projects attracted both forest fire and deforestation. Of the total area in settlement projects, 40% was affected by forest fires and 17% was deforested. Rivers are particularly important for deforestation in this part of Amazonia, and efforts to protect forest along the rivers are therefore necessary. The ability to predict where deforestation and fires are most likely to occur is important for designing policies for preventative actions.

Keywords: land-cover change; extreme drought; wildfire; forest degradation; Amazon forest; forest fire.

1 Introduction

Forest fire and deforestation are the main threats to the Amazon forest. In 2020, an area of 10,897 km^2 of forest was cleared and the cumulative area of forest loss in Brazil's Legal Amazon region reached 820,000 km² (INPE, 2021). In 2016 the annual loss of forest carbon from degradation represented 38% of the total forest carbon loss in Brazilian Amazonia and 47% of the total in the Amazon basin as a whole (Walker et al., 2020). Degradation of standing forest by logging and fire in Amazonia is much less studied and understood than deforestation.

Most forest degradation by fire in the Brazilian Amazon occurs when fires escape control and spread from pasture into the forest. In the last decade, fires affected millions of hectares of Amazon forest, emitting large amounts of carbon to the atmosphere and reducing biomass carbon stocks (Barbosa and Fearnside, 1999; Fonseca et al., 2017; Vasconcelos et al., 2013). During the 2015 drought, the number of forest fires in the Brazilian Amazon increased by 36% compared to the previous 12 years and the mean annual of emission by forest fires was 454 Tg CO_2 or 31% of the estimated emissions from deforestation (Aragão et al., 2018).

Forest fire in the Amazon is mainly associated with two factors, land-use and cover change (e.g., conversion of forest to pasture) and extreme drought events (e.g., El Niño and the Atlantic Multidecadal Oscillation), the first factor being a source of ignition and the second a condition making the forest more flammable and increasing the impacts of fire when it occurs (Alencar et al., 2006; Cano-Crespo et al., 2015). The main ignition source of forest fires is slash-and-burn to clear land for agricultural and cattle ranching and the use of fire for maintenance of areas in agriculture and especially pasture (Aragão et al., 2008, 2014). The cause of extreme droughts in the central Amazon is attributed to El Niño events (Aragao et al., 2007), and strong El Niños have become more prevalent in recent decades and are predicted to become even more frequent in the future, making the forest still more susceptible to fire (Cai et al., 2014; Yeh et al., 2009). Projections of climate change in the future indicate that there will be an increase in precipitation in the rainy season and a decrease in the dry season. It is also predicted that the temperature will rise constantly during the dry seasons (Oo et al., 2019). The combined effect of higher temperature and dryer conditions exceeds the limits of tolerance of many Amazon trees, resulting in mortality (Fearnside, 2015; Phillips et al., 2009). The expected increase in severe droughts in the Amazon makes it urgent to understand their potential impacts on forests.

During the 1997/98 El Niño, approximately 1000 km^2 of forest was burned along the Madeira and Purus Rivers (Nelson, 2001). This is an area located in the central Amazon, where the areas of upland forests (*terra firme*) have some of the highest biomass densities in the Amazon (382 – 385 Mg ha^{-1}), which gives this area a great potential for carbon-stock loss by fire and deforestation (Nogueira et al., 2015). Fire is most frequent in the area known as the “arc of deforestation” in the southern and eastern portions of the Amazon, where land-use and cover change is most intense. However, with the increased frequency of extreme El Niño events, forest fires can spread into large areas of forest in the central Amazon, even though the flammability of the forest under “normal” environmental conditions is low (Nepstad et al., 2004).

The development of strategies to avoid degradation by forest fires and deforestation requires understanding the dynamics of the drivers that control their occurrence spatially and through time. These drivers differ in different parts of the Amazon forest, making it necessary to have information from each part of this vast region (Fearnside, 2008, 2017). The climatic and economic conditions that favor forest degradation are better understood than are the landscape variables. Understanding which variables in the landscape can influence the occurrence of forest fire and deforestation in central Amazonia is crucial for creating policies to prevent and combat these forest-degradation sources. Our hypotheses are that the area of burned forest is increasing over time and that anthropogenic, biophysical and land-category variables can influence the occurrence of forest fire and deforestation. The aims of the present study were to estimate the area of forest burned over time and to assess the potential drivers (anthropogenic, biophysical and land-category variables) that could contribute to deforestation and forest fires in the central Brazilian Amazon.

2 Materials and Methods

2.1 Study area

The study was carried out in the municipality (county) of Autazes, in the state of Amazonas, Brazil. Autazes is bounded to the north by the Amazon River and to the east by the Madeira River (IBGE, 2018). AM-254 is the main highway in the municipality, connecting the city of Autazes to Highway BR-319 (Manaus-Porto Velho) at km 18, thus providing a connection to Manaus, the capital of Amazonas State (Figure 1). The total area of Autazes is 763,226 ha (one-third the size of Wales) and this municipality is the largest milk and cheese producer in Amazonas State, both for bovine cows and water buffalo. Autazes has the largest water-buffalo herd among the 62 municipalities in Amazonas State and the bovine herd is the ninth largest (Almudi and Pinheiro, 2015). Annual rainfall is between 2000 and 2400 mm, with three months of precipitation less than 100 mm (Sombroek, 2001), and the mean annual temperature is 27ºC (White, 2018). The predominant soil type is yellow ferralsol (IBGE and EMBRAPA, 2001), and the vegetation type that covers most of the area is dense-canopy rainforest on non-flooding lowlands (IBGE code: Da) (SIPAM, 2002). There did not appear to have been any significant disturbance from logging, which is important because previous logging is known to be an important factor in increasing the vulnerability of Amazon forest to fire (Berenguer et al., 2014; Condé et al., 2019; Nepstad et al., 1999).

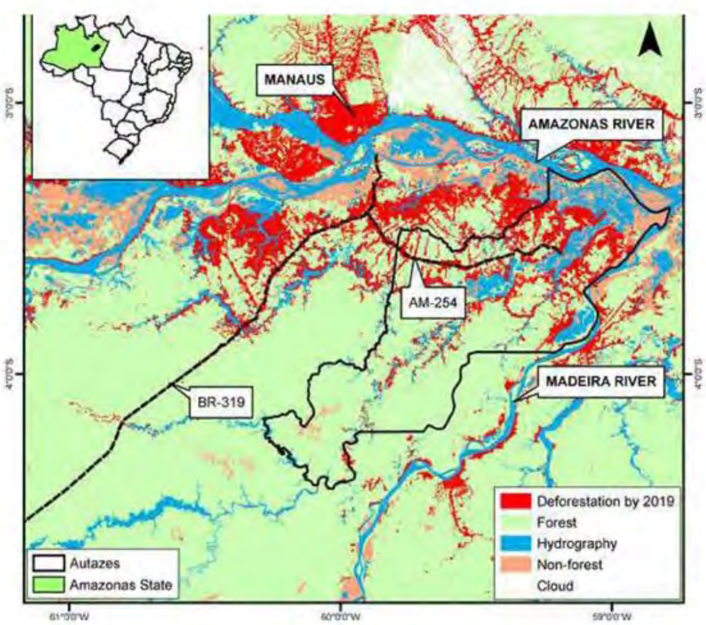

Figure 1: Location of the municipality of Autazes.

2.2 Methodological approach

The steps in the methodology are illustrated in the flowchart below (Figure 2). First we acquired and prepared the dataset needed for the analysis. These data are composed of anthropogenic, biophysical and land-category variables, together with data on precipitation and “hot pixels” (cells in the satellite image grid where the thermal channel of the sensor is saturated, often indicating presence of a fire in the cell). We then performed an exploratory analysis comparing this information with our map of forest fires. Lastly we calculated the weights-of-evidence contrast, used to analyze the relationship between our variables and the occurrence of forest fires and deforestation.

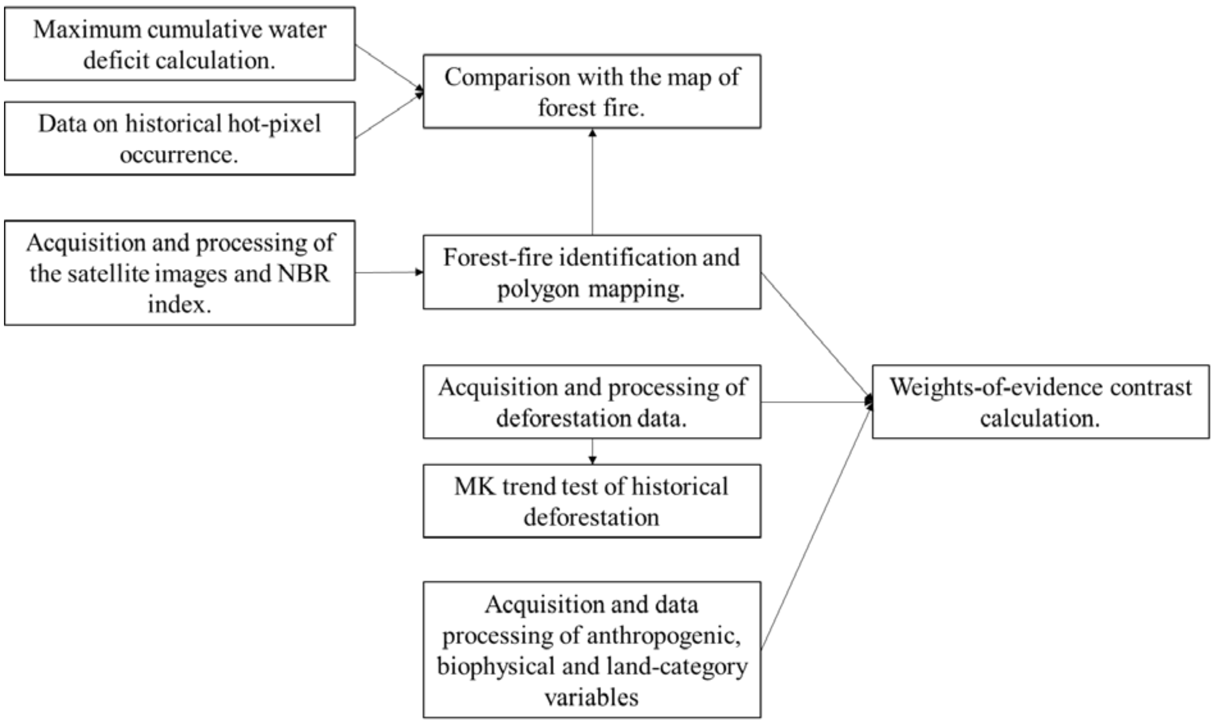

Figure 2: Flowchart of the methodology followed during the study.

2.3 Forest burn-scar mapping

The forest burn scars were mapped for a period of 31 years (1985-2015) by visual interpretation at a scale of 1:15,000 using satellite images from Landsat 5-TM, Landsat 8-OLI (spatial resolution 30 m) and Resourcesat-1- LISS III, which has an original spatial resolution of 23.5 m that we resized to 30 m (Table S1 in the Supplementary Material). The images were obtained during the dry season (June to September) and the images with the lowest cloud cover were selected. The projection used was Universal Transverse Mercator (UTM), Datum World Geodetic System 1984 (WGS 84), in the South 21 zone.

Burn scars were identified and mapped in the forest areas using maps of the delta normalized burn ratio (dNBR) and a color composition of the shortwave infra-red (SWIR), near infra-red (NIR) and red (R) bands (Figure S1). More detail about the dNBR method is available in the Supplementary Material.

A fire that occurs in a specific year is detected in the subsequent year because there can be a delay of up to one year for the burn scar to be detectable on satellite images. Thus, a burn scar mapped at time (t + 1) is attributed to the previous year (t) in order to represent the real year of the fire (Vasconcelos et al., 2013).

The scars of burned forest can be identified because the dry leaves and twigs from tree mortality reflect most in the SWIR spectral band due to their containing less moisture than unburned forest. A part of the SWIR radiation is absorbed by the water, thereby reducing the release of radiation from objects with high moisture (Key and Benson, 2006; Ponzoni et al., 2012; Veraverbeke et al., 2011). We validated the mapped burn scars based on GPS (Global Positioning System) points collected during the field work in the study area (October 2017). We collected a total of 120 points, of which 49 were from burned forest areas and 71 were from unburned forest areas. The global accuracy score was 0.80, a value considered to be very good by previous studies (e.g., Landis and Koch, 1977).

We used hot-pixel data from 1998 to 2015 to evaluate possible fire ignition and its relationship with forest fires. These datasets are available from the Queimadas Project on the INPE platform (http://www.inpe.br/queimadas/portal). Understory forest fires usually cannot be detected by hot pixels, although fires can be easily detected in the case of slash-and-burn and burning for maintenance of agriculture and pasture areas -- the main ignition sources for forest fire (Alencar et al., 2015; Silvestrini et al., 2011).

2.4 Calculation of maximum cumulative water deficit

We evaluated forest climatic conditions as related to drought severity by using Maximum Cumulative Water Deficit (MCWD), which is estimated based on the difference between precipitation and forest evapotranspiration (Equations S1, S2 and S3). MCWD values were estimated following the studies by Aragão et al. (2007) and Saatchi et al. (2013). Calculation of drought severity using precipitation data has been shown to be efficient (Abdulrazzaq et al., 2019).We assessed the severity of the dry season each year (1996 to 2015) by selecting the month in each year with the highest value of cumulative water deficit (CWD). Precipitation data were obtained from pluviometric station 00359004 of the National Water Agency (ANA), located in the city of Autazes. These data are available on the Hidroweb online platform (http://www.snirh.gov.br/hidroweb/apresentacao). We selected the month with the highest *CWD* value in the year (i.e., the *MCWD*) to evaluate the severity of the dry season for each year.

2.5 Deforestation data and anthropogenic, biophysical and land-category variables

The vector map of deforestation was obtained from the Project for Monitoring Amazonian Deforestation (PRODES) (INPE, 2021). We separated the deforestation polygons based on spatial location: (i) “under the influence of rivers” for polygons located within 2 km of rivers and (ii) “under the influence of roads” for polygons located within 2 km of either main or secondary roads. We chose a 2-km limit because the forest in these polygons is most attractive for deforestation (Barber et al, 2014; Fearnside et al., 2009). Deforestation in the overlap zone between the road and river buffers was considered separately in this analysis because we could not identify which of these drivers was influencing deforestation occurrence the most.

We developed maps of a group of variables: roads (mapped visually for each year from 1997 to 2018), watercourses (extracted from PRODES), rural settlements (National Institute of Colonization and Agrarian Reform - INCRA), indigenous lands (National Indian Foundation - FUNAI), slope and elevation (Shuttle Radar Topographic Mission -

SRTM), soils (Brazilian Institute of Geography and Statistics - IBGE) and forest type (Amazon Protection System - SIPAM). We used this group of variables to understand the behavior of forest fire and deforestation, both of which were mapped.

2.6 Statistical analysis

The dynamics of deforestation were analyzed annually from 2001 to 2018. Before 2000 the polygons (map areas enclosing a given feature) represent cumulative deforestation. We used the Mann-Kendall trend test to assess the existence and direction of a significant trend in deforestation. This trend test has been used by previous studies to detect trends in historical environmental data (Moreira and Naghettini, 2016; Silva Junior et al., 2017; Souza et al., 2011). This test was applied using the mk.test function in the Trend Package in R software. The null hypothesis was that there is no trend and the alternative hypothesis was that there is a trend in the data. Positive values of z indicate an upward trend and negative values indicate a downward trend.

To analyse the influence of anthropogenic, biophysical and land-category variables on forest fires and deforestation occurrence in Autazes, we used the weights-of-evidence contrast (WOEC) statistic. This is a Bayesian statistic that determines the probability of an event occurring based on evidence factors (Bonham-Carter et al., 1989). The WOEC is calculated considering a transition between categories on the maps and a group of variables. The transitions in our study were from forest to deforestation and from forest to burned forest. The group of static variables was the same for both transitions, except that the forest-fire scar map was part of the group of variables used to analyze deforestation. We selected this variable because it could influence the occurrence of land-cover change (Barber et al., 2014; White, 2018).

Positive values of weights-of-evidence indicate attraction for the occurrence of events such as deforestation and forest fires, while these events are inhibited when the values are negative. Values close to zero mean that there are no effects on these events. The higher a positive value is, the greater the attraction, and the greater the magnitude of a negative value the stronger the repulsion (Soares-Filho et al., 2009). In the WOEC approach the maps analyzed should be spatially independent; to assess independence between the variables we used the Cramer test and the point information uncertainty test (Soares-Filho et al., 2009). Values greater than 0.5 indicate that the pair of variables is spatially dependent. This threshold has been used by previous studies to evaluate the dependence between variables that influence deforestation (Almeida et al., 2005; Yanai et al., 2012). None of our variables showed spatial dependency, and we therefore maintained all variables in the analysis. All of these procedures were performed in Dinamica EGO 5 software, which is freely available for download at http://csr.ufmg.br/dinamica/.

To calculate the WOEC of forest fires, we used the map before the fire occurrence as the initial map and the map after the fire occurrence as the final map. For deforestation in burned-forest areas we used the landscape map for the year following the forest fire as the initial map and the map for the image three years after the forest fire as the final landscape map (Table 1).

Year of landscape maps	Transitions	Variables		
		Anthropogenic	**Biophysical**	**Land categories**
1998 to 2000 2010 to 2012 2016 to 2018	Forest to Deforestation	- Distance from roads - Distance from deforestation - Areas of forest fire	- Distance from rivers - Forest type - Soil type - Slope - Elevation	- Rural settlement - Indigenous Land
1997 2009 2015	Forest to Burned forest	- Distance from roads - Distance from deforestation	- Distance from rivers - Forest type - Soil type - Slope - Elevation	- Rural settlement - Indigenous Land

Table 1: Variables that could influence in the forest fire and deforestation occurrence used to calculate the weights-of-evidence contrast according to different transitions.

3 Results

3.1 History of forest-fire scars

Out of a total of 31 years (1985-2015), forest fires were found in three years: 1997, 2009 and 2015 (Figure 3). The areas of forest burned were 45,724 ha (1997), 9432 ha (2009) and 28,171 ha (2015), representing, respectively, 9%, 2% and 6% of total forest cover in the study area. Out of the total area of forest burned (83,327 ha), 67,282 ha (81%) was forest burned once, 14,316 ha (17%) burned twice, and 1729 ha (2%) burned three times. Forest in the northern portion of the municipality of Autazes burned in all three years. The wildfires mapped in 2015 were more spread out than in previous years (1997 and 2009), and they were mainly associated with deforestation along the rivers (Figure 3).

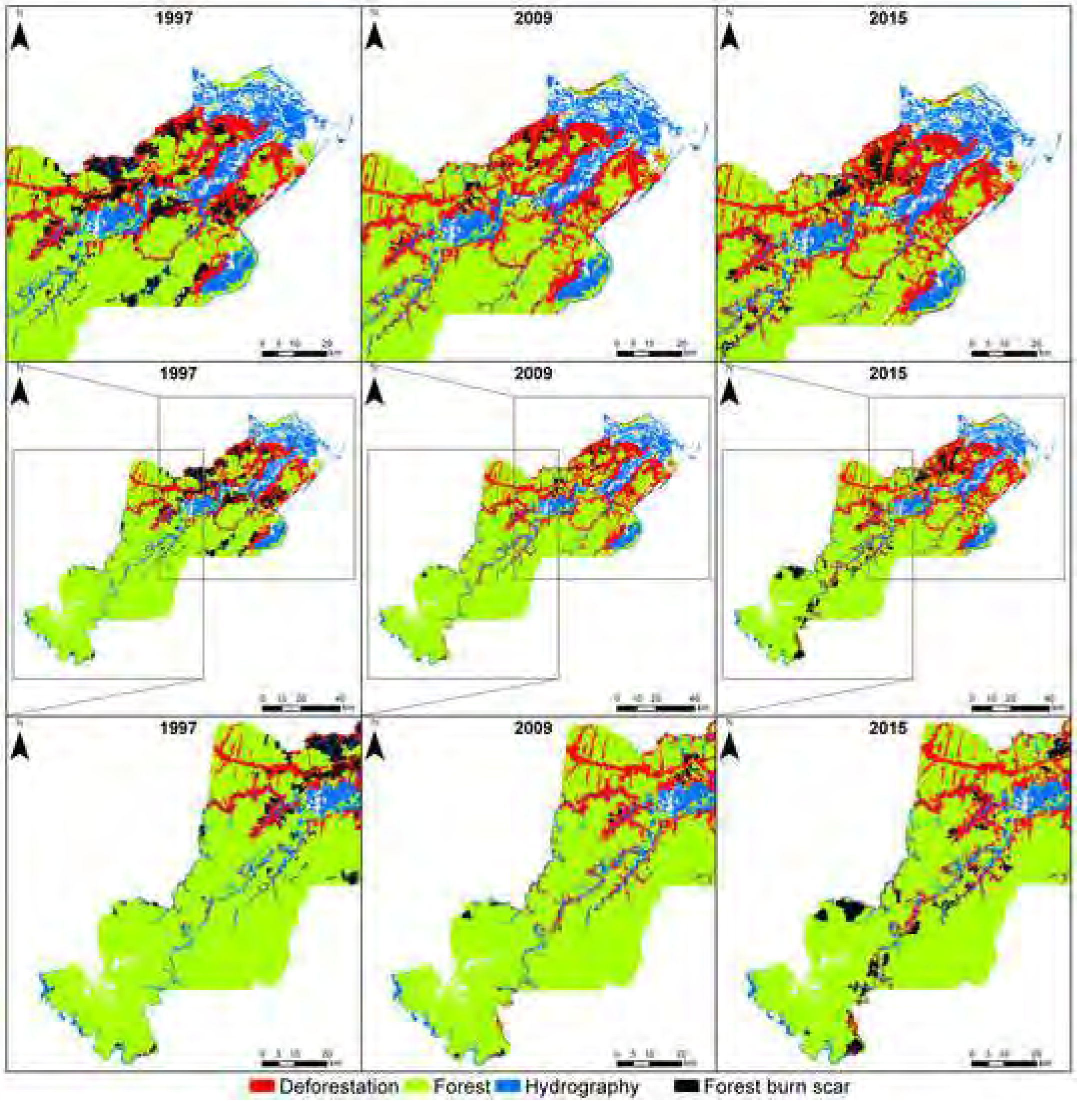

Figure 3: Deforestation and forest burn scars in the municipality of Autazes in 1997, 2009 and 2015.

The area of burned forest in Indigenous land in the municipality represented 3.4% of the total forest burned in the time period analyzed (1985 to 2015). Of the forest in Indigenous land, 14% was burned during the study period. Settlement projects of all types, accounted for 13.5% of the total forest area burned in the municipality during the study period, and 52% of the forest in the settlement projects burned.

3.2 Hot-pixel occurrence and maximum cumulative water deficit

Since 2009 we observed a substantial increase in the number of hot pixels in Autazes, where 300 hot pixels were identified in 2015 (Figure S2). This is the highest number of hot pixels in any year since these data began to be recorded in 1998 and is roughly double the number of hot pixels in the second and third-ranking years for hot-pixel occurrence (2014 and 2010). Although hot pixels occurred in forest areas during normal years (i.e., not El Niño years), we could not identify the presence of forest burn scars in the areas surrounding these pixels. Out of a total of 19 years (1996-2015) of data on maximum cumulative water deficits, the years with MCWD values with the largest magnitudes were 1997 (-327.8 mm), 2009 (-263.3 mm) and 2015 (-339.2 mm) (Figure S3). The average MCWD for the years without extreme-drought events was -159.5.

3.3 Deforestation

Deforestation through 2018 in Autazes totaled 134,188 ha, or 17.5% of the total area of the municipality. Of the deforestation total, 99% (132,410 ha) was located within a 2-km buffer from roads and rivers. Considering the same distances, 62.3% of the deforestation was located along the rivers, 12.7% along the roads and 25.0% in the overlap between these two buffer areas (Table 2).

Deforestation (ha) from 2000 to 2018							
Buffer Distance	Rivers	%	Roads	%	Overlap between roads and rivers	%	Total
2 km	82,547.0	62.3	16,987.5	12.7	32,965.2	25.0	132,409.7

Table 2: Estimates of deforestation considering the rivers and roads and the area of overlap between the buffers.

Historic deforestation in the municipality of Autazes showed a downward trend according to the Mann-Kendall trend test (total in 2-km buffer: $z = -2.309$, $p = 0.02094$). Although the deforestation trend from 2000 t 2018 was similar near rivers and roads, deforestation in the river buffer showed an increase between 2003 and 2005, while the deforestation near roads decreased in this period. From 2006 to 2007 the rate of deforestation near rivers was almost constant, while it increased along the roads; between 2009 and 2010 deforestation decreased close to rivers and increased near roads (Table 2).

Of the total of deforestation in 2000, 2001 and 2002, 22.7% (3030.1 ha) was located in forest areas that burned in 1997. In 2010, 2011 and 2012, 6% (266.1 ha) of the deforestation was in forests burned in 2009. For 2016, 2017 and 2018, 11% (417.5 ha) of the deforestation was in areas of forest burned in 2015. In relation to the percentage of burned forest that was subsequently deforested, 6.6% was clearing of the forest that burned in 1997, 2.8% of the forest that burned in 2009 and 1.5% of the forest that burned in 2015. From 2000 to 2018 deforestation in Indigenous land represented 2% of the total deforestation, and that in settlement projects represented 17% of the total deforestation in Autazes. During the same period, 5% of the forest in Indigenous land was deforested and 24% of the forest in settlement projects.

3.4 Effect of landscape variables on forest-fire and deforestation occurrence

In terms of the occurrence of forest fire, the pattern of the values for WOEC was similar for the variables "distance from deforested areas" and "distance from rivers" in the three drought years (1997, 2009 and 2015). Areas close to previous deforestation and close to rivers showed positive values of WOEC, indicating that these areas were more attractive to forest-fire occurrence (Figure 4A). The "distance to roads" variable had positive values in all three years in the area up to 3000 m from the roads (Figure 4B). For 1997 the values had a downward trend with increasing distance, as expected, but for 2009 the values were almost constant and for 2015 the values increased with greater distance from roads. The effect of distance to rivers declined with distance, as expected (Figure 4C).

For the slope variable, we found that areas with high slope values had a higher chance of forest-fire occurrence than areas with low values for all three years analyzed (Figure 4D). The presence of a rural settlement favored forest-fire occurrence in 1997. In contrast, the presence of Indigenous land inhibited forest fire for the three years analyzed (Figure 4E and F).

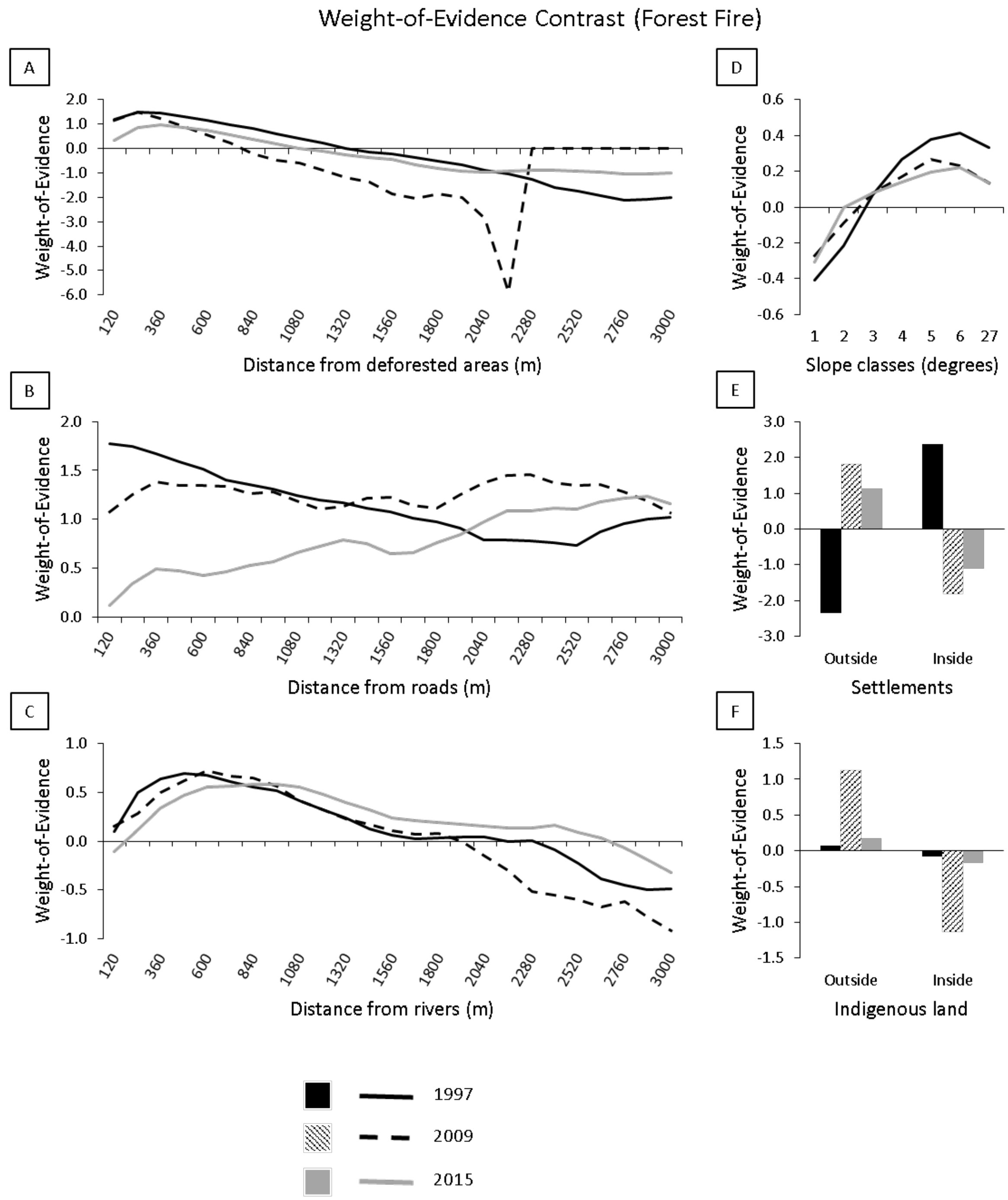

Figure 4: Weights-of-evidence contrast of variables that influence forest-fire occurrence in the study area. (A) Distance from deforested areas, (B) Distance from roads, (C) Distance from rivers, (D) Slope classes (degrees), (E) Settlement projects and (F) Indigenous land.

The WOEC values for elevation were only positive in the interval between 21 m and 40 m for forest-fire occurrence in all years (1997, 2009 and 2015) (Figure S4a). The type of forest most susceptible to forest-fire occurrence was dense-canopy rainforest on non-flooding lowlands (Db), which had positive values of WOEC in the analyzed years

(1997, 2009 and 2015). In contrast, dense-canopy rainforest on river floodplains (Da) was not susceptible, with negative values for all of the three years (Figure S5a). In terms of soil type, only the red-yellow acrisols had positive values, while the values were variable between the three years on other soil types (Figure S6a).

In relation to deforestation, the WOEC values for all three years (1997, 2009 and 2015) indicated that areas close to previous deforestation and to roads and rivers were more favorable to being deforested in comparison to more-distant areas (Figure 5). Within 600 m of the previously deforested areas the WOEC values were positive for the occurrence of new deforestation. The influence of roads increases the occurrence of deforestation up to a distance of approximately 900 m, and the positive influence of the rivers on deforestation extends for about 1200 m. Areas in rural settlement only had positive values of WOEC for deforestation in 1997. For all three years with forest fire the areas of forest that had been burned were more favorable to being deforested later than were areas of intact forest. In contrast to settlement projects, Indigenous land inhibited deforestation occurrence (Figure 5).

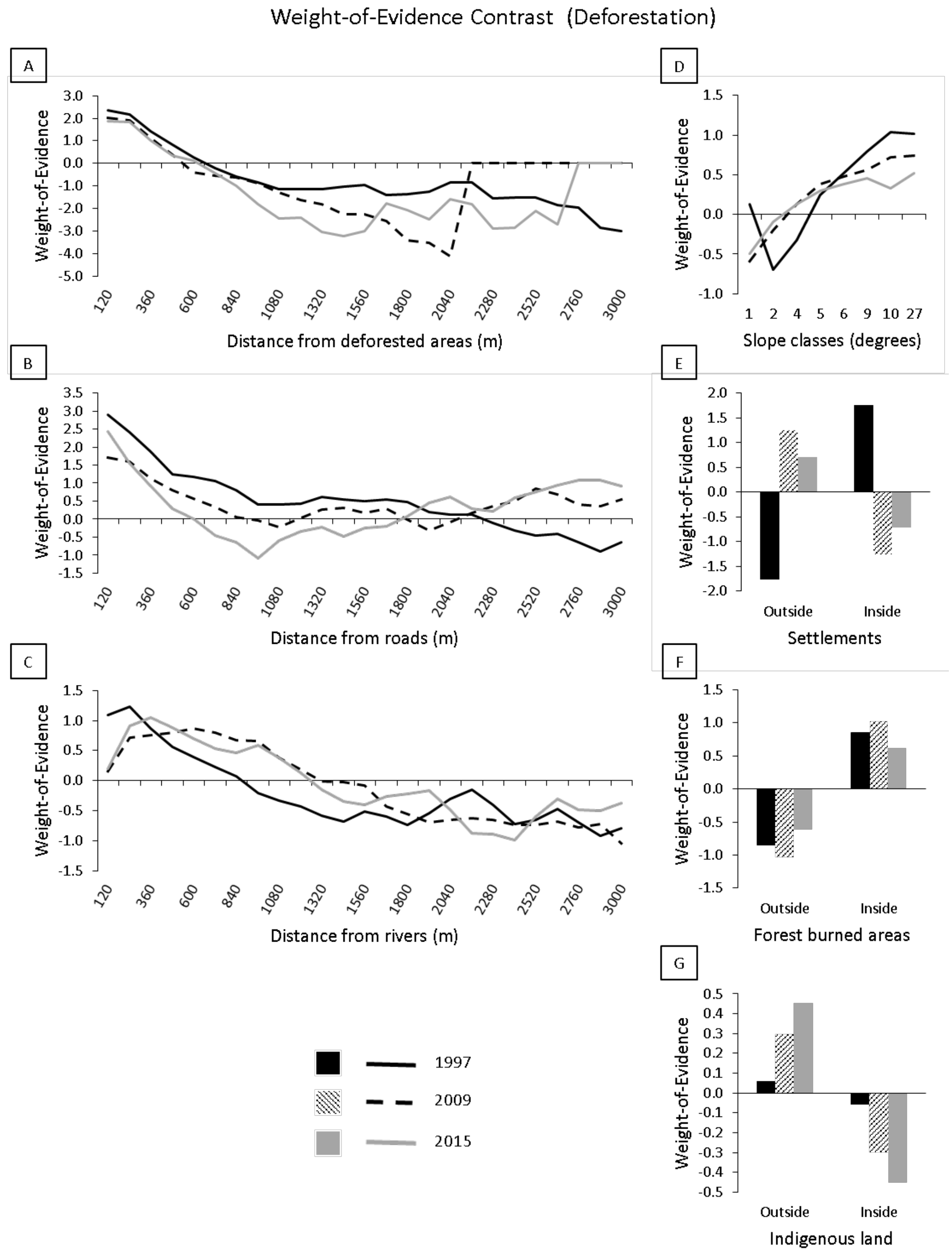

Figure 5: Weights-of-evidence contrast of variables that influence the occurrence of deforestation. (A) Distance to deforested areas, (B) Distance to roads, (C) Distance to rivers, (D) Slope classes (degrees), (C) Settlement projects, (F) Burned-forest areas and (G) Indigenous land. For settlements, Indigenous land and burned-forest areas, “outside” and “inside” refer to the limits of these areas.

We did not observe a clear tendency in the relation of elevation to deforestation (Figure S4b), although the WOEC values for the years 2009 and 2015 were similar at different levels of elevation. The forest types that were most attractive for being cleared were secondary forest (Vs) and open-canopy rainforest on non-flooding lowlands (Ab), followed by dense-canopy rainforest on river floodplains (Da). Dense-canopy rainforest on non-flooding lowlands (Db) had negative values in two of the three years analyzed (1997 and 2009) (Figure S5b). The WOEC values for different soil types did not show a well-defined pattern for deforestation occurrence in the years analyzed (1997, 2009 and 2015) (Figure S6b).

4 Discussion

4.1 Forest-fire dynamics

In the three years that forest burn scars were mapped (1997, 2009 and 2015), severe droughts caused by El Niño affected the Amazon forest, making the forest susceptible to wildfires (Jiménez-Muñoz et al., 2016; Marengo and Espinoza, 2016). The El Niño in 1997/98 and 2015/16 were considered to be the strongest in the last thirty years (Jiménez-Muñoz et al., 2016). The large values for water deficit in these years reveal the intensity of the droughts. These droughts caused severe impacts on the forest, increasing tree mortality. Dry dead trees are ideal fuels for fire, and their presence makes the forest flammable and susceptible to large wildfires (Nepstad et al., 2004). Our hypothesis that the forest-fire area is increasing over time was not supported, although the projected increase in severe El Niño events may make such a pattern emerge in the future. Forest fires in this part of Amazonia are only occurring in extreme El Niño years and the area burned is proportional to the severity of the fires. This information implies the need to create policies to prevent the use of the fire in pasture management in these years, and to intensify oversight to discourage illegal use of fire. Action is needed to provide incentives for implementation of agriculture and pasture with fire-free techniques.

In 1997/98 large areas of forest burned in Amazonia, including 23,341 km² in Roraima (Barbosa and Fearnside, 1999), 39,000 km² in Pará and Mato Grosso (Alencar et al., 2006) and approximately 1000 km² in the central Amazon (Nelson, 2001). The area of forest burn scars mapped in 2009 was smaller than the area in 1997/98, which could be related to the fact that the drought in 2009 was less severe than in 1997 and 2015. In addition, in 2009 the change from El Niño to La Niña occurred after a short period of time. This change increased rainfall in the central Amazon (including Autazes), reducing the drought effect (Kim et al., 2011; Marengo et al., 2012). The fact that wildfires could not be detected in our study area during the drought years caused by the Atlantic Multidecadal Oscillation (AMO) in 2005 and 2010 (Lewis et al., 2011; Marengo et al., 2008) is consistent with the attribution of the droughts that occurred in the central Amazon to El Niño rather than to the AMO (Aragão et al., 2007).

Burned forest is more susceptible to new wildfires than unburned forest (Cochrane and Schulze, 1999). In Autazes 19% of the burned forest had been affected by more than one forest-fire event. Out of this total, 17% had burned twice and 2% had burned three times. The majority of the area of wildfire burned only once, which was the same pattern found by Morton et al. (2013). Therefore, the small amount of overlap that occurred over time was probably due to the great dispersion of the ignition sources. In addition, the interval between the forest-fire events could have allowed regeneration of forests located in upland areas (Flores et al., 2014), which was the type of forest that was most impacted by fire in the municipality.

4.2 Deforestation dynamics

Deforestation in Brazilian Amazonia as a whole has been mainly in the “arc of deforestation" on the southern and eastern edges of the region, where it is associated with the road network, deforested areas having expanded based on the increase of main and secondary roads (Barber et al., 2014; Fearnside and Graça, 2006). However, in the case of the municipality of Autazes, we found that 62% of the deforestation was located along rivers, indicating the importance of hydrography (watercourses) in the dynamics of land-use and cover change in the area. The river banks were the first areas occupied by the local population, and almost all parts of Autazes can be accessed by navigable rivers. The distribution of deforestation in the municipality is closely linked to the traditional lifestyle of the people known as “*ribeirinhos*,” who live on the river banks and use this space for agriculture and livestock. In addition, this region was widely occupied by Mura indigenous people who traditionally live dispersed along the lakes and large rivers and, more recently, in areas close to smaller rivers (Canalez et al., 2017; Pereira, 2016).

Areas that are periodically flooded (known as *várzeas*) along sediment-laden white-water rivers like the Madeira and the Amazon are attractive to agriculture and cattle ranching because soil fertility is higher due to the deposition of sediments originating in the Andes (Cravo et al., 2002; Junk et al., 2012). During the part of the year when the river flow is low, the herds are taken to pastures in the *várzeas*, where there is an abundance of high-quality native grass. During the flood period, the herds are moved to the *terra firme* (unflooded uplands), in general to pastures located along the roads (Cravo et al., 2002). The “high” *várzeas* are those areas that stay flooded for less than three months of the year (Junk et al., 2012; Wittmann et al., 2002), thus allowing the herds to spend most of the year in this *várzea* area. The pasture area in the *várzeas* is therefore larger than that located along the roads, where the cattle stay for a shorter time.

Although burned-forest areas are susceptible to deforestation, in our study area the percentage of burned forest that was deforested was small (6.6%, 2.8% and 1.5% for forest burned in 1997, 2009 and 2015, respectively), indicating that little of the burned forest is deforested in the years following the fire. In southern Amazonia between 1999 and 2007, only 1% of the burned-forest area was deforested within 3 years of a fire, and between 1999 and 2005 3.8% of the burned-forest area was deforested (Morton et al., 2013). In dense forests in the eastern Amazon, 6% of the burned areas were subsequently deforested, and the deforestation of burned forest did not explain the total deforestation ($p=0.63$) (Alencar et al., 2015). This supports the conclusion that the forest fires are caused by fire accidentally escaping from established pastures when these areas are burned to renew the grass and to control invading woody vegetation, rather than by fires being set to deliberately degrade the forest to facilitate or help legalize deforestation.

4.3 Effect of landscape variables on land-cover change

For all variables analyzed the behavior was similar for both deforestation and forest fires. However, a slight difference was observed in the values of the WOEC. Areas deforested previously, roads and navigable rivers are all attractive for these events: the closer a given area is to these features, the greater the probability that these events will occur. Roads and navigable rivers are the main means of access to intact forest in Amazonia (Barber et al., 2014; Fearnside, 1987; Laurance et al., 2002). Forests close to previously deforested areas are attractive to deforestation because of agricultural expansion. In terms of forest fires, the distance that the fire penetrated into the forest from deforested areas was greater for the years with the highest values for maximum cumulative water deficit (1997 and 2015), followed by the year with the lowest value (2009). With drier weather, fires that are used for pasture maintenance can spread into forest more easily (Alencar et al., 2006; Cano-Crespo et al., 2015; Fonseca et al., 2017).

The values of WOEC between slope and forest fire are positive because steeper slopes allow fire to spread more quickly and easily. Steeper slope facilitates fire spread because it brings the flames into closer contact with to the unburned fuel, resulting in faster and more effective pre-heating (Finney et al., 2015). This positive relationship between slope and fire spread has also been found in a mountainous region in southeastern Brazil (Santos et al., 2019). The municipality of Autazes as a whole has little variability in slope, since the relief is relatively flat with smooth undulations, which means that the slope effect would not be a prominent factor for forest fire in the large flat areas (Gonçalves Júnior, 2013). However, both forest fire and deforestation in the municipality are concentrated in river-bank areas where the in slope is higher (Bispo et al., 2009; Flores et al., 2017; Resende et al., 2014). This explains why the WOEC values between slope and forest fire were positive in our study. It also explains why our deforestation data show the relationship with slope as positive, which is the opposite of what occurs in regions with steep slopes, with steep areas being avoided for deforestation because of their lower agricultural potential (e.g., Santos et al., 2019). Although the WOEC showed that areas of forest that were burned are more susceptible to being deforested, we found that only a small percentage of the burned-forest area was subsequently deforested. This also occurs in other parts of the Amazon, and through the years the pattern of deforestation and forest fire have shown differences, where in some years deforestation rates decreased and the forest-fire rates increased (Aragão et al., 2018; Cano-Crespo et al., 2015).

By 1997 the municipality of Autazes had only one “traditional” settlement project (PA: *projeto de assentamento federal*) (INCRA, 2017). In this type of rural settlement the area is divided in lots and the main activity is cattle ranching, resulting in large amounts of clearing (Yanai et al., 2017). From 2004 to 2005 three agro-extractivist settlement projects (PAEs: *projetos de assentamento agroextrativista*) were created (INCRA, 2017). In this type of settlement the families that are settled are supposed to focus their activity on harvesting non-timber forest products, resulting is low deforestation pressure (Yanai et al., 2017). Fire tends to occur more in the PA settlement type, where agriculture and cattle ranching activities are more intense as compared to the PAE settlement type.

In the municipality of Autazes there is only one type of protected area, in this case Indigenous land. Most of the clearing found in Indigenous land occurred before 1999 in the six Indigenous lands that existed at the time, which had a total area of only 5215 ha. Subsequently eight more Indigenous lands were created (2001, 2003, 2006, 2011, 2015 and 2016) totaling 88,602 ha. In 2018 the cumulative deforestation in Indigenous land represented just 2% of the total area, showing the effectiveness of Indigenous areas in controlling the spread of deforestation. All of these areas are traditionally occupied by Indigenous people. The environmental preservation of Indigenous lands is important for the survival of the Indigenous people (FUNAI, 2020; Nepstad et al., 2006).

Dense-canopy rainforest on non-flooding lowlands (Db) is the predominant forest type in the municipality and is the one that covers most of the areas close to roads, rivers and urban areas. Many agricultural areas are located close to this forest type, and the fire used for maintenance is the main ignition source for wildfire. This explains why this type of forest was the vegetation type most affected by fire. In contrast, we did not find forest fires in dense-canopy rainforest on river floodplains (Da) because most forest of this type had already been deforested.

The forest type for which deforestation pressure was highest was the "open-canopy rainforest on non-flooding lowlands," even though this forest type only occurs in a small patch in the municipality. Pressure was high because of its proximity to the city of Autazes and to agricultural areas. In the case of forest fires, the forest type most attractive to this disturbance was "dense-canopy rainforest on non-flooding lowlands," even though this forest type was not attractive for deforestation. This behavior shows that forest fire can occur even without the occurrence of deforestation, indicating that if the forest is burned the area may not be more likely to be converted to deforestation.

Secondary forests (Vs) were attractive to clearing, which reflects the fact that these areas are repeatedly cleared. However, the values for clearing secondary forests are not counted as "deforestation" by INPE's PRODES deforestation-monitoring program, which only considers deforestation to occur once at any given location. The PRODES deforestation data therefore represent an underestimate of the total rate of clearing (Aragão et al., 2018; Tasker and Arima, 2016).

Our results suggest that both forest fire and deforestation occur in proximity to deforested areas, roads and rivers, and these features have more influence on the likelihood of clearing than do the characteristics of the forest type. The same holds for the soil type, where deforestation and fire are more closely related to proximity to previous deforestation, roads and rivers than to the physical and chemical characteristics of soils.

5 Conclusions

Deforestation is strongly linked to rivers where human occupation predominates, and the occurrence of forest fires is related with the extreme drought caused by El Niño in the municipality of Autazes. Since extreme-drought events are expected to become more frequent in the future, forest fires can be expected to have a crucial role in the loss of forest biomass. Forest fires in Autazes are more closely related to maintenance of agriculture and ranching using fire that can escape into forest, rather than to deforestation of new areas. The landscape variables that most explained the behavior of both deforestation and forest fires were the distances from deforested areas, roads and rivers. Indigenous land had an important role in protecting forest, while settlements projects favored deforestation and fire as expected, especially in the settlement project of the "traditional" (PA) type. Of the total area in settlement projects of all types, 40% was burned and17% was deforested during the study period (1985-2018). These results can contribute to creating more effective measures to combat deforestation and especially forest fires because results such as these make it possible to identify priority areas for preventative actions.

Abbreviations

AMO Atlantic Multidecadal Oscillation
ANA National Water Agency
CWD cumulative water deficit
dNBR delta normalized burn ratio
GPS global positioning system
FUNAI National Indian Foundation
IBGE Brazilian Insitute for Geography and Statistics
INCRA National Institute for Colonization and Agrarian Reform
INPE National Institute for Space Research
MCWD maximum cumulative water deficit
NBR normalized burn ratio
NIR near infra-red
PA federal settlement project
PAE agroextractivist settlement project
PRODES Project for Monitoring Amazonian Deforestation
SIPAM Amazon Protection System
SRTM Shuttle Radar Topographic Mission
SWIR shortwave infra-red
WOEC weights-of-evidence contrast

Acknowledgments

We thank the National Institute of Amazonia Research (INPA PRJ15.125), the National Institute of Science and Technology for Environmental Services of Amazonia (INCT-SERVAMB), the National Council for Scientific and Technological Development (CNPq, processes 610042/2009-2 and 313107/2013-0), the Foundation for Support of Research of Amazonas State (FAPEAM, process 708565) and the Coordination of Personnel Improvement at the Superior Level (CAPES).

6 References

Abdulrazzaq, Z.T., Hasan, R.H., Aziz, N.A., 2019. Integrated TRMM data and standardized precipitation index to monitor the meteorological drought. Civ. Eng. J. 5, 1590–1598. https://doi.org/10.28991/cej-2019-03091355

Alencar, A., Nepstad, D., Diaz, M.C.V., 2006. Forest Understory fire in the Brazilian Amazon in ENSO and non-ENSO years: Area burned and committed carbon emissions. Earth Interact. 10, 1–17. https://doi.org/10.1175/EI150.1

Alencar, A.A., Brando, P.M., Asner, G.P., Putz, F.E., 2015. Landscape fragmentation, severe drought, and the new Amazon forest fire regime. Ecol. Appl. 25, 1493–1505. https://doi.org/10.1890/14-1528.1

Almeida, C.M., Vieira Monteiro, A.M., Câmara, G., Soares-Filho, B.S., Coutinho Cerqueira, G., Lopes Pennachin, C., Batty, M., 2005. GIS and remote sensing as tools for the simulation of urban land-use change. Int. J. Remote Sens. 26, 759–774. https://doi.org/10.1080/01431160512331316865

Almudi, T., Pinheiro, J.O.C., 2015. Dados Estatísticos da Produção Agropecuária e

Florestal do Estado do Amazonas: Ano 2013. Embrapa Amazônia Ocidental, Manaus, AM, Brazil. https://bityl.co/5PmG

Aragao, L., Malhi, Y., Roman-Cuesta, R.M., Saatchi, S., Anderson, L.O., Shimabukuro, Y.E., Aragão, L.E.O.C., 2007. Spatial patterns and fire response of recent Amazonian droughts. Geophys. Res. Lett. 34, 1–5. https://doi.org/10.1029/2006gl028946

Aragão, L.E.O.C., Anderson, L.O., Fonseca, M.G., Rosan, T.M., Vedovato, L.B., Wagner, F.H., Silva, C.V.J., Silva Junior, C.H.L., Arai, E., Aguiar, A.P., Barlow, J., Berenguer, E., Deeter, M.N., Domingues, L.G., Gatti, L., Gloor, M., Malhi, Y., Marengo, J.A., Miller, J.B., Phillips, O.L., Saatchi, S., 2018. 21st Century drought-related fires counteract the decline of Amazon deforestation carbon emissions. Nat. Commun. 9, 1–12. https://doi.org/10.1038/s41467-017-02771-y

Aragão, L.E.O.C., Malhi, Y., Barbier, N., Lima, A., Shimabukuro, Y., Anderson, L., Saatchi, S., 2008. Interactions between rainfall, deforestation and fires during recent years in the Brazilian Amazonia. Philos. Trans. R. Soc. B Biol. Sci. 363, 1779–1785. https://doi.org/10.1098/rstb.2007.0026

Aragão, L.E.O.C., Poulter, B., Barlow, J.B., Anderson, L.O., Malhi, Y., Saatchi, S., Phillips, O.L., Gloor, E., 2014. Environmental change and the carbon balance of Amazonian forests. Biol. Rev. 89, 913–931. https://doi.org/10.1111/brv.12088

Barber, C.P., Cochrane, M.A., Souza, C.M., Laurance, W.F., 2014. Roads, deforestation, and the mitigating effect of protected areas in the Amazon. Biol. Conserv. 177, 203–209. https://doi.org/10.1016/j.biocon.2014.07.004

Barbosa, R.I., Fearnside, P.M., 1999. Incêndios na Amazônia Brasileira: estimativa da emissão de gases do efeito estufa pela queima de diferentes ecossistemas de Roraima na passagem do evento “El Nino” (1997/98). Acta Amaz. 29, 513–534. https://doi.org/10.1590/1809-43921999294534

Berenguer, E., Ferreira, J., Gardner, T.A., Aragão, L.E.O.C., de Camargo, P.B., Cerri, C.E., Durigan, M., de Oliveira Jr., R.C., Vieira, I.C.G., Barlow, J., 2014. A large-scale field assessment of carbon stocks in human-modified tropical forests. Global Change Biol. 20, 3713–3726, https://doi.org/10.1111/gcb.12627

Bispo, P. da C., Valeriano, M. de M., Kuplich, T.M., 2009. Variáveis geomorfométricas locais e sua relação com a vegetação da região do interflúvio Madeira-Purus (AM-RO). Acta Amaz. 39, 81–90. https://doi.org/10.1590/S0044-59672009000100008

Bonham-Carter, G.F., Agterberg, F.P., Wright, D.F., 1989. Weight of evidence modelling: a new approach to mapping mineral potential, in: Statistical Applications in the Earth Sciences. pp. 171–183. https://doi.org/10.4095/128059

Canalez, G. de G., Silva, F.F., Noda, S. do N., 2017. Conhecer para conservar: Caracterização da comunidade Boa Esperança, Autazes/AM. Areté 10, 1–11.

Cano-Crespo, A., Oliveira, P.J.C., Boit, A., Cardoso, M., Thonicke, K., 2015. Forest edge burning in the Brazilian Amazon promoted by escaping fires from managed pastures. J. Geophys. Res. Biogeosciences 120, 2095–2107. https://doi.org/10.1002/2015JG002914

Cochrane, M.A., Schulze, M.D., 1999. Fire as a recurrent event in tropical forests of the eastern Amazon: Effects on forest structure, biomass, and species composition. Biotropica 31, 2–16. https://doi.org/10.1111/j.1744-7429.1999.tb00112.x

Condé, T.M., Higuchi, N., Lima, A.J.N., 2019; Illegal selective logging and forest fires in the northern Brazilian Amazon. Forests 10, art. 61. https://doi.org/10.3390/f10010061

Cravo, M. da S., Xavier, J.J.B.N., Dias, M.C., Barreto, J.F., 2002. Características, uso agrícola atual e potencial das várzeas no Estado do Amazonas, Brasil. Acta Amaz. 32, 351–365. https://doi.org/10.1590/1809-43922002323365

de Souza, F.D.A.S., de Morais, H.F., da Silva, V.D.P.R., 2011. Influência da Urbanização no Clima da cidade de Campina Grande - PB. Rev. Bras. Geogr. Física 16(1), 134–145. https://doi.org/10.1590/s1678-86212016000100058

Fearnside, P.M., 1987. Deforestation and International Economic Development Projects in Brazilian Amazonia. Conserv. Biol. 1, 214–221. https://doi.org/10.1111/j.1523-1739.1987.tb00035.x

Fearnside, P.M., 2008. The roles and movements of actors in the deforestation of Brazilian Amazonia. Ecology and Society 13(1), art. 23. http://www.ecologyandsociety.org/vol13/iss1/art23/

Fearnside, P.M., 2017. Deforestation of the Brazilian Amazon. Oxford Research Encyclopedia of Environmental Science. https://doi.org/10.1093/acrefore/9780199389414.013.102

Fearnside, P.M., 2019. Amazônia e o aquecimento global. *Amazônia Real*. https://bityl.co/5QI2

Fearnside, P.M., Graça, P.M.L.A., 2006. BR-319: Brazil's Manaus-Porto Velho Highway and the potential impact of linking the arc of deforestation to central Amazonia. Environ. Manage. 38, 705–716. https://doi.org/10.1007/s00267-005-0295-y

Finney, M.A., Cohen, J.D., Forthofer, J.M., McAllister, S.S., Gollner, M.J., Gorham, D.J., Saito, K., Akafuah, N.K., Adam, B.A., English, J.D., Dickinson, R.E., 2015. Role of buoyant flame dynamics in wildfire spread. Proc. Natl. Acad. Sci. U. S. A. 112, 9833–9838. https://doi.org/10.1073/pnas.1504498112

Flores, B.M., Holmgren, M., Xu, C., van Nes, E.H., Jakovac, C.C., Mesquita, R.C.G., Scheffer, M., 2017. Floodplains as an Achilles' heel of Amazonian forest resilience. Proc. Natl. Acad. Sci. 114, 4442–4446. https://doi.org/10.1073/pnas.1617988114

Flores, B.M., Piedade, M.T.F., Nelson, B.W., 2014. Fire disturbance in Amazonian blackwater floodplain forests. Plant Ecol. Divers. 7, 319–327. https://doi.org/10.1080/17550874.2012.716086

Fonseca, M.G., Anderson, L.O., Arai, E., Shimabukuro, Y.E., Xaud, H.A.M., Xaud, M.R., Madani, N., Wagner, F.H., Aragão, L.E.O.C., 2017. Climatic and anthropogenic drivers of northern Amazon fires during the 2015-2016 El Niño event. Ecol. Appl. 27, 2514–2527. https://doi.org/10.1002/eap.1628

FUNAI (Fundação Nacional do Índio), 2020.Demarcação de Terras. https://bityl.co/5Qwh (accessed 6 June 2020).

Gonçalves Júnior, E.S., 2013. Terraços Fluviais Quaternários das Regiões de Careiro da Várzea, Manaquiri, Careiro Castanho e Autazes, Amazônia Central.

IBGE (Instituto Brasileiro de Geografia e Estatística), 2018. Cidades. http://cidades.ibge.gov.br/painel/historico (accessed 13 January 2018).

IBGE (Instituto Brasileiro de Geografia e Estatística); EMBRAPA (Empresa Brasileira de Pesquisa Agropecuária), 2001. Mapa de Solos do Brasil. Rio de Janeiro: IBGE, 2001 - Escala 1:5.000.000. https://bityl.co/5Qvw (accessed 7 October 2020).

INCRA (Instituto Nacional de Colonização e Reforma Agrária), 2017. Incra nos Estados - Informações gerais sobre os assentamentos da Reforma Agrária. http://painel.incra.gov.br/sistemas/index.php (accessed 6 June 2020).

INPE (Instituto Nacional de Pesquisas Espaciais), 2020. Incrementos de desmatamento -

Amazônia Legal - estados. https://bityl.co/5Qx1 (accessed 8 February 2020).

Jiménez-Muñoz, J.C., Mattar, C., Barichivich, J., Santamaría-Artigas, A., Takahashi, K., Malhi, Y., Sobrino, J.A., Van Der Schrier, G., 2016. Record-breaking warming and extreme drought in the Amazon rainforest during the course of El Niño 2015-2016. Sci. Rep. 6, 1–7. https://doi.org/10.1038/srep33130

Junk, W.J., Piedade, M.T.F., Schöngart, J., Wittmann, F., 2012. A classification of major natural habitats of Amazonian white-water river floodplains (várzeas). Wetl. Ecol. Manag. 20, 461–475. https://doi.org/10.1007/s11273-012-9268-0

Key, C.H., Benson, N.C., 2006. Landscape Assessment (LA): Sampling and Analysis Methods, in: FIREMOM: Fire Effects Monitoring and Inventory System. p. LA-1-LA-55. https://bityl.co/5Plu

Kim, W., Yeh, S.-W., Kim, J.-H., Kug, J.-S., Kwon, M., 2011. The unique 2009-2010 El Niño event: A fast phase transition of warm pool El Niño to La Niña. Geophys. Res. Lett. 38, 1–5. https://doi.org/10.1029/2011GL048521

Landis, J., Koch, G. G. 1997. The measurements of observer agreement for categorical data. Biometrics. 33, 159-174. https://doi.org/10.2307/2529310

Laurance, W.F., Albernaz, A.K.M., Schroth, G., Fearnside, P.M., Bergen, S., Venticinque, E.M., da Costa, C., 2002. Predictors of deforestation in the Brazilian Amazon. J. Biogeogr. 29, 737–748. https://doi.org/10.1046/j.1365-2699.2002.00721.x

Lewis, S.L., Brando, P.M., Phillips, O.L., van der Heijden, G.M.F., Nepstad, D., 2011. The 2010 Amazon drought. Science 331, 554–554. https://doi.org/10.1126/science.1200807

Marengo, J.A., Espinoza, J.C., 2016. Extreme seasonal droughts and floods in Amazonia: causes, trends and impacts. Int. J. Climatol. 36, 1033–1050. https://doi.org/10.1002/joc.4420

Marengo, J.A., Nobre, C.A., Tomasella, J., Oyama, M.D., Sampaio de Oliveira, G., de Oliveira, R., Camargo, H., Alves, L.M., Brown, I.F., 2008. The drought of Amazonia in 2005. J. Clim. 21, 495–516. https://doi.org/10.1175/2007JCLI1600.1

Marengo, J.A., Tomasella, J., Soares, W.R., Alves, L.M., Nobre, C.A., 2012. Extreme climatic events in the Amazon basin. Theor. Appl. Climatol. 107, 73–85. https://doi.org/10.1007/s00704-011-0465-1

Moreira, J.G. do V., Naghettini, M., 2016. Detecção de Tendências Monotônicas Temporais e Relação com Erros dos Tipos I e II: Estudo de caso em séries de precipitações diárias máximas anuais do Estado do Acre. Rev. Bras. Meteorol. 31, 394–402. https://doi.org/10.1590/0102-778631231420140155

Morton, D.C., Le Page, Y., DeFries, R., Collatz, G.J., Hurtt, G.C., 2013. Understorey fire frequency and the fate of burned forests in southern Amazonia. Philos. Trans. R. Soc. B Biol. Sci. 368, art. 20120163. https://doi.org/10.1098/rstb.2012.0163

Nelson, B.W., 2001. Fogo em florestas da Amazônia Central em 1997. An. X SBSR, pp. 1675–1682. https://bityl.co/5Pm1

Nepstad, D.C., Lefebvre, P., Lopes da Silva, U., Tomasella, J., Schlesinger, P., Solorzano, L., Moutinho, P., Ray, D., Benito, J.G., 2004. Amazon drought and its implications for forest flammability and tree growth: a basin-wide analysis. Glob. Chang. Biol. 10, 704–717. https://doi.org/10.1111/j.1529-8817.2003.00772.x

Nepstad, D.C., Verissimo, A., Alencar, A., Nobre, C., Lima, E., Lefebvre, P., Schlesinger, P., Potter, C., Moutinho, P., Mendoza, E., Cochrane, M., Brooks, V., 1999. Large-

scale impoverishment of Amazonian forests by logging and fire. Nature 398, 505-508. https://doi.org/10.1038/19066
Nepstad, D.C., Schwartzman, S., Bamberger, B., Santilli, M., Ray, D., Schlesinger, P., Lefebvre, P., Alencar, A., Prinz, E., Fiske, G., Rolla, A., 2006. Inhibition of Amazon Deforestation and fire by parks and Indigenous lands. Conserv. Biol. 20, 65–73. https://doi.org/10.1111/j.1523-1739.2006.00351.x
Nogueira, E.M., Yanai, A.M., Fonseca, F.O.R., Fearnside, P.M., 2015. Carbon stock loss from deforestation through 2013 in Brazilian Amazonia. Glob. Chang. Biol. 21, 1271–1292. https://doi.org/10.1111/gcb.12798
Oo, H.T., Zin, W.W., Thin Kyi, C.C., 2019. Assessment of Future Climate Change Projections Using Multiple Global Climate Models. Civ. Eng. J. 5, 2152–2166. https://doi.org/10.28991/cej-2019-03091401
Pereira, M.L. de C., 2016. Território e mobilidade Mura no baixo rio Madeira (AM). Habitus 14(2), 263–275. https://doi.org/10.18224/hab.v14.2.2016.263-275
Phillips, O.L. & 65 others, 2009. Drought sensitivity of the Amazon rainforest. *Science*, 323, 1344-1347. http://doi.org/10.1126/science.1164033
Ponzoni, F.J., Shimabukuro, Y.E., Kuplich, T.M., 2012. Sensoriamento Remoto da Vegetação, 2ª edição. ed. Oficina de Textos, São Paulo.
Resende, A.F., Nelson, B.W., Flores, B.M., de Almeida, D.R., 2014. Fire Damage in seasonally flooded and upland forests of the central Amazon. Biotropica 46, 643–646. https://doi.org/10.1111/btp.12153
Saatchi, S., Asefi-Najafabady, S., Malhi, Y., Aragao, L.E.O.C., Anderson, L.O., Myneni, R.B., Nemani, R., 2013. Persistent effects of a severe drought on Amazonian forest canopy. Proc. Natl. Acad. Sci. 110, 565–570. https://doi.org/10.1073/pnas.1204651110
Santos, J.F.C., Gleriani, J.M., Velloso, S.G.S., Souza, G.S.A., Amaral, C.H., Torres, F.T.P., Medeiros, N.D.G., Reis, M., 2019. Wildfires as a major challenge for natural regeneration in Atlantic Forest. Sci. Total Environ. 650, 809–821. https://doi.org/10.1016/j.scitotenv.2018.09.016
Silva Junior, C.H.L., Aragão, L.E.O.C., Anderson, L.O., 2017. Tendências temporais do número de queimadas na Amazônia Legal brasileira entre os anos de 2002 a 2014. An. XVIII Simpósio Bras. Sensoriamento Remoto 654–661.
Silvestrini, R.A., Soares-Filho, B.S., Nepstad, D., Coe, M., Rodrigues, H., Assunção, R., 2011. Simulating fire regimes in the Amazon in response to climate change and deforestation. Ecol. Appl. 21, 1573–1590. https://doi.org/10.1890/10-0827.1
SIPAM (Sistema de Proteção da Amazônia), 2002. Mapa de Vegetação do Brasil- Escala 1:250.000. https://bityl.co/5QxO (accessed 7 October 2020)
Soares-Filho, B.S., Rodrigues, H.O., Costa, W.L., 2009. Modeling environmental dynamics with Dinamica EGO, Instituto de Geociências - Centro de Sensoriamento Remoto. https://doi.org/10.13140/RG.2.1.5179.4641
Sombroek, W., 2001. Spatial and Temporal Patterns of Amazon Rainfall. AMBIO A J. Hum. Environ. 30, 388–396. https://doi.org/10.1579/0044-7447-30.7.388
Tasker, K.A., Arima, E.Y., 2016. Fire regimes in Amazonia: The relative roles of policy and precipitation. Anthropocene 14, 46–57. https://doi.org/10.1016/j.ancene.2016.06.001
van Marle, M.J.E., Field, R.D., van der Werf, G.R., Estrada de Wagt, I.A., Houghton, R.A., Rizzo, L. V., Artaxo, P., Tsigaridis, K., 2017. Fire and deforestation dynamics in

Amazonia (1973–2014). Global Biogeochem. Cycles 31, 24–38. https://doi.org/10.1002/2016GB005445

Vasconcelos, S.S., Fearnside, P.M., Graça, P.M.L.A., Nogueira, E.M., de Oliveira, L.C. Figueiredo, E.O., 2013. Forest fires in southwestern Brazilian Amazonia: Estimates of area and potential carbon emissions. For. Ecol. Manage. 291, 199–208. https://doi.org/10.1016/j.foreco.2012.11.044

Veraverbeke, S., Harris, S., Hook, S., 2011. Evaluating spectral indices for burned area discrimination using MODIS/ASTER (MASTER) airborne simulator data. Remote Sens. Environ. 115, 2702–2709. https://doi.org/10.1016/j.rse.2011.06.010

White, B.L.A., 2018. Spatiotemporal variation in fire occurrence in the state of Amazonas, Brazil, between 2003 and 2016. Acta Amaz. 48, 358–367. https://doi.org/10.1590/1809-4392201704522

Wittmann, F., Anhuf, D., Funk, W.J., 2002. Tree species distribution and community structure of central Amazonian várzea forests by remote-sensing techniques. J. Trop. Ecol. 18, 805–820. https://doi.org/10.1017/S0266467402002523

Yanai, A.M., Fearnside, P.M., Graça, P.M.L.A., Nogueira, E.M., 2012. Avoided deforestation in Brazilian Amazonia: Simulating the effect of the Juma Sustainable Development Reserve. For. Ecol. Manage. 282, 78–91. https://doi.org/10.1016/j.foreco.2012.06.029

Yanai, A.M., Nogueira, E.M., de Alencastro Graça, P.M.L., Fearnside, P.M., 2017. Deforestation and carbon stock loss in Brazil's Amazonian settlements. Environ. Manage. 59, 393–409. https://doi.org/10.1007/s00267-016-0783-2

SUPPLEMENTARY MATERIAL

Forest Fires and Deforestation in the Central Brazilian Amazon: Effects of Landscape and Climate on Spatial and Temporal Dynamics

Delta normalized burn ratio (dNBR)

The dNBR refers to a technique for change detection based on subtraction of NBR values before a wildfire from the corresponding values after the fire. The NBR is an index determined by the ratio of the difference between the NIR and SWIR 2 bands and the sum of these values (Equation S1). This index is used in wildfire mapping because it highlights the burned-forest areas. The color composition used was of the SWIR, NIR and R bands in the red (R), green (G) and blue (B) channels. This composition allows identifying burned-forest areas (magenta color) and unburned-forest areas (green color) (Figure S1a). While the color composition is better for identifying these areas, the dNBR map is better for determining the limits visually (Figure S1b).

The images used for dNBR were obtained from the Earth Resources Observation and Science (EROS) Center Science Processing Architecture (ESPA) platform of United States Geological Survey (USGS).

Equation to calculate the Normalized Burn Ratio (NBR):

$$NBR = \frac{NIR - SWIR\,2}{NIR + SWIR\,2} \quad (1)$$

Where *NBR* is the normalized burn ratio, *NIR* is the near infra-red band and *SWIR2* is the shortwave infra-red 2 band.

Equations to calculate cumulative water deficit:

If $WD_{n-1} - E_n + P_n < 0\,;$ (2)

Then, $CWD_n = WD_{n-1} - E_n + P_n < 0\,;$ (3)

If not $WD_n = 0$ (4)

Where, *WD* is the monthly water deficit when evapotranspiration is greater than precipitation. *E* is the forest evapotranspiration of 100 mm per month and *P* is the monthly precipitation. *CWD* is the cumulative water deficit that corresponds to the sum of consecutive *WD* values.

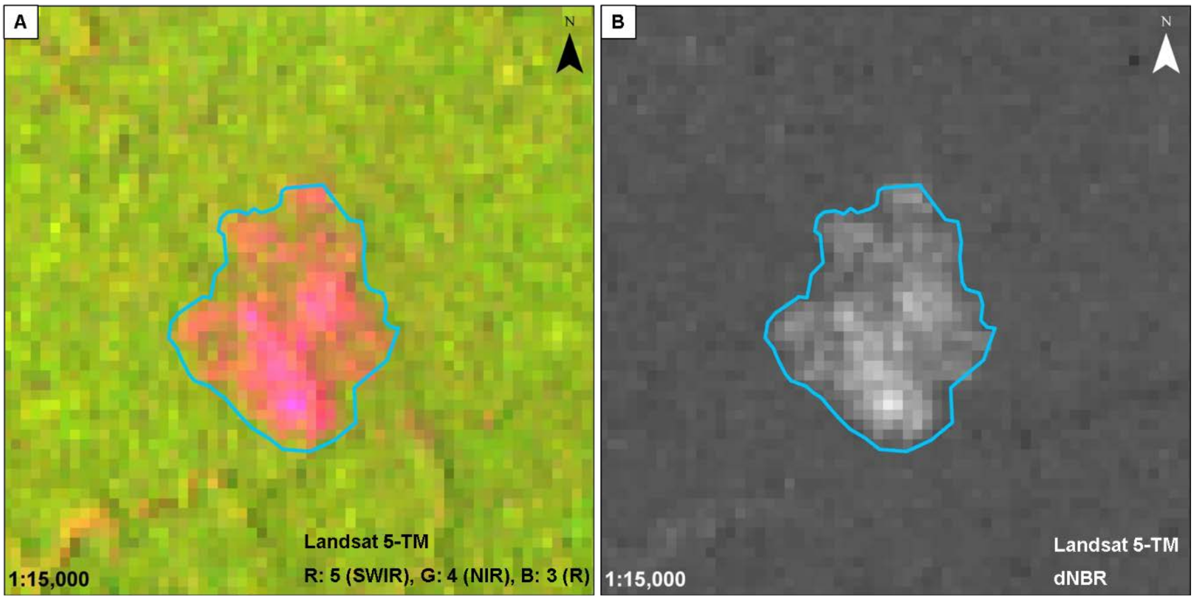

Figure S1: Mapping of a burned-forest area using a Landsat 5-TM image (A) Color composition with the forest in green and the burn scar in magenta and (B) dNBR index mapped from the image with forest in darker shades of gray and the burn scar in lighter shades of gray.

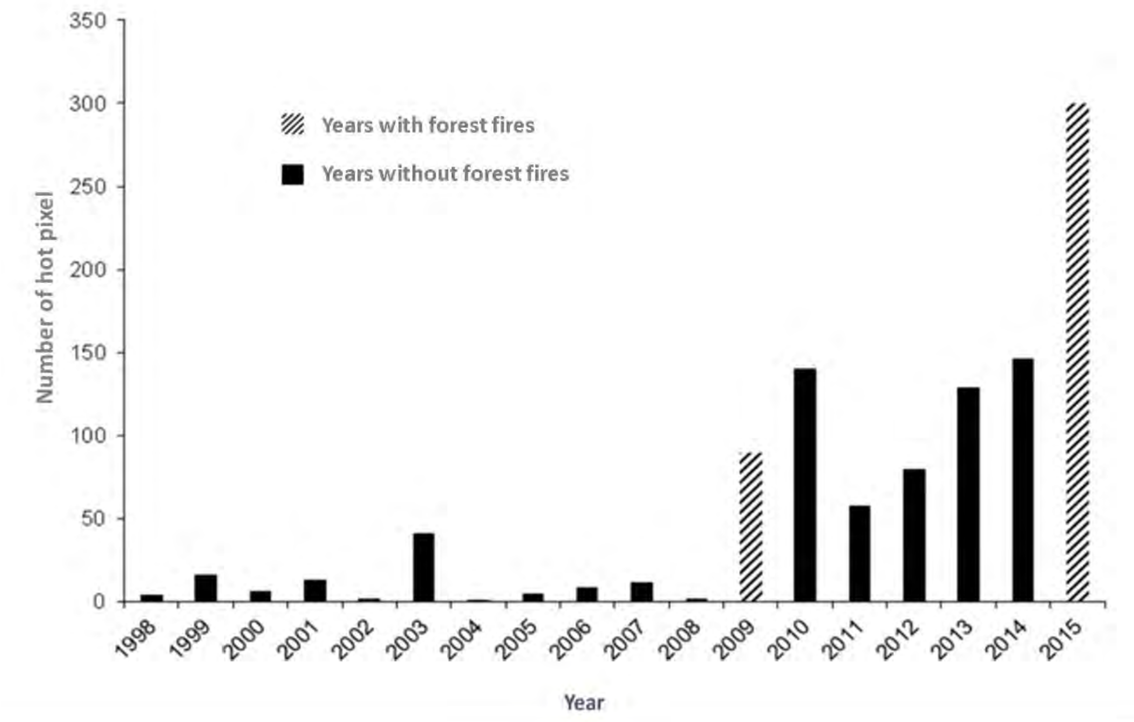

Figure S2: Historic of hot pixels occurrence in municipality of Autazes. Solid bars represent hot pixels in years without wildfire occurrence, and hatched bars represent years when hot pixels and wildfires occurred.

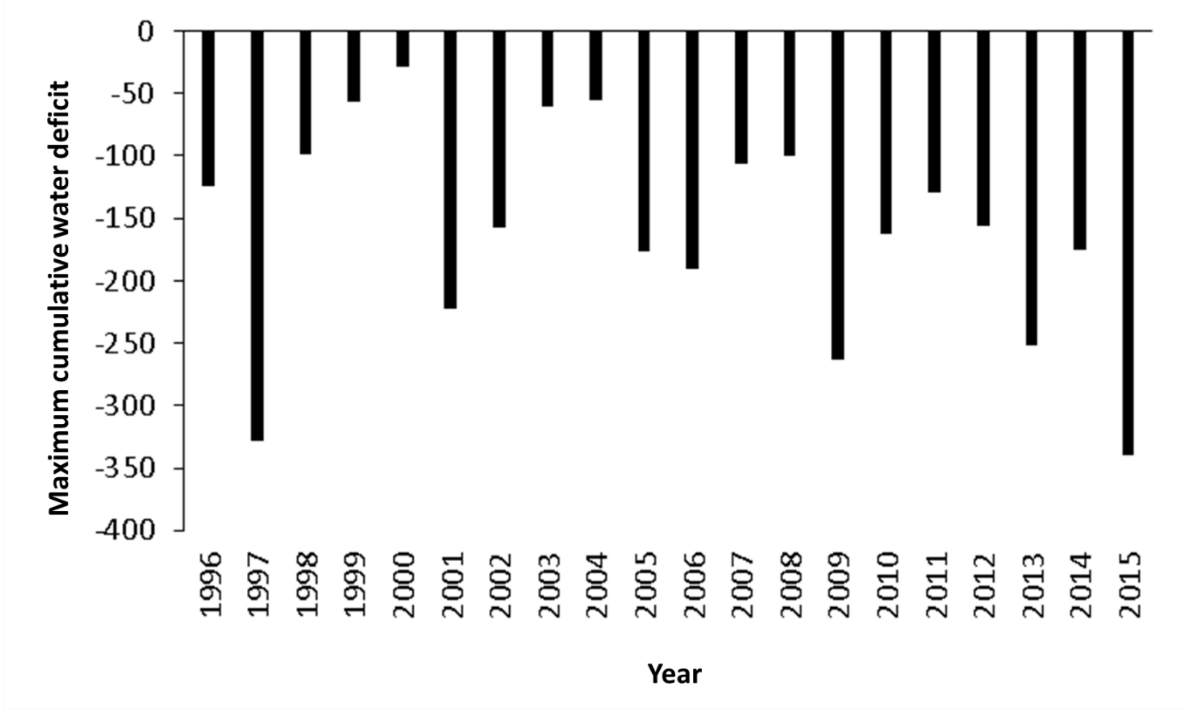

Figure S3: Maximum cumulative water deficit (MCWD) from 1996 to 2015.

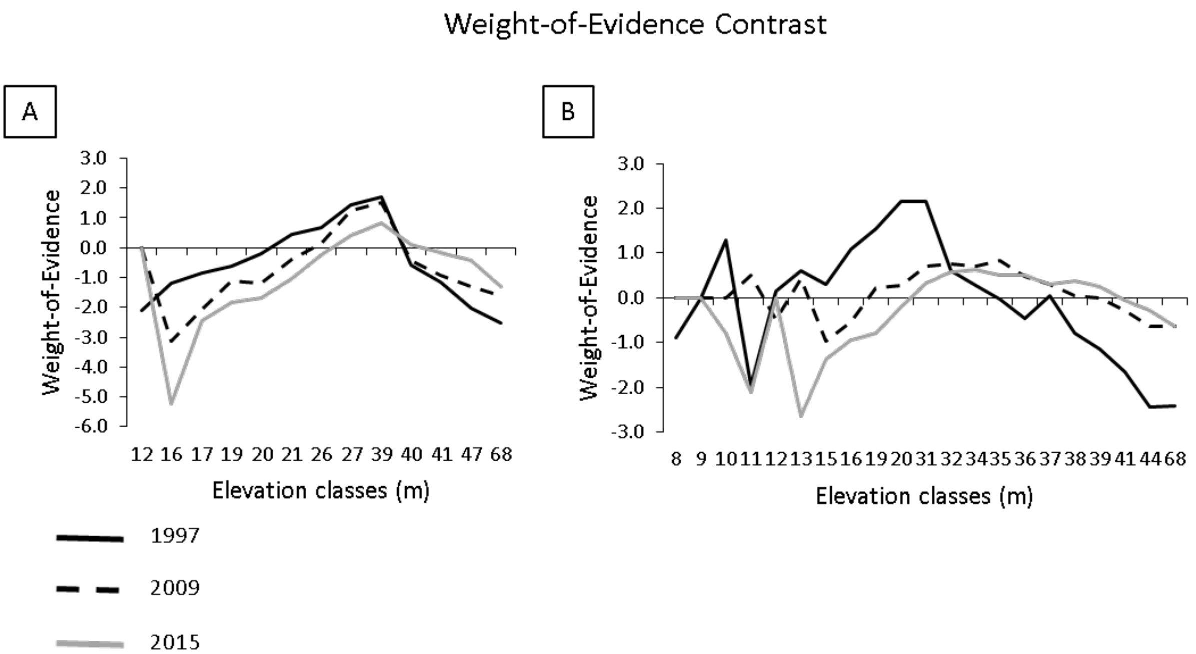

Figure S4: Behavior of weights-of-evidence contrasts over the range of elevation classes for (A) Forest fire and (B) Deforestation.

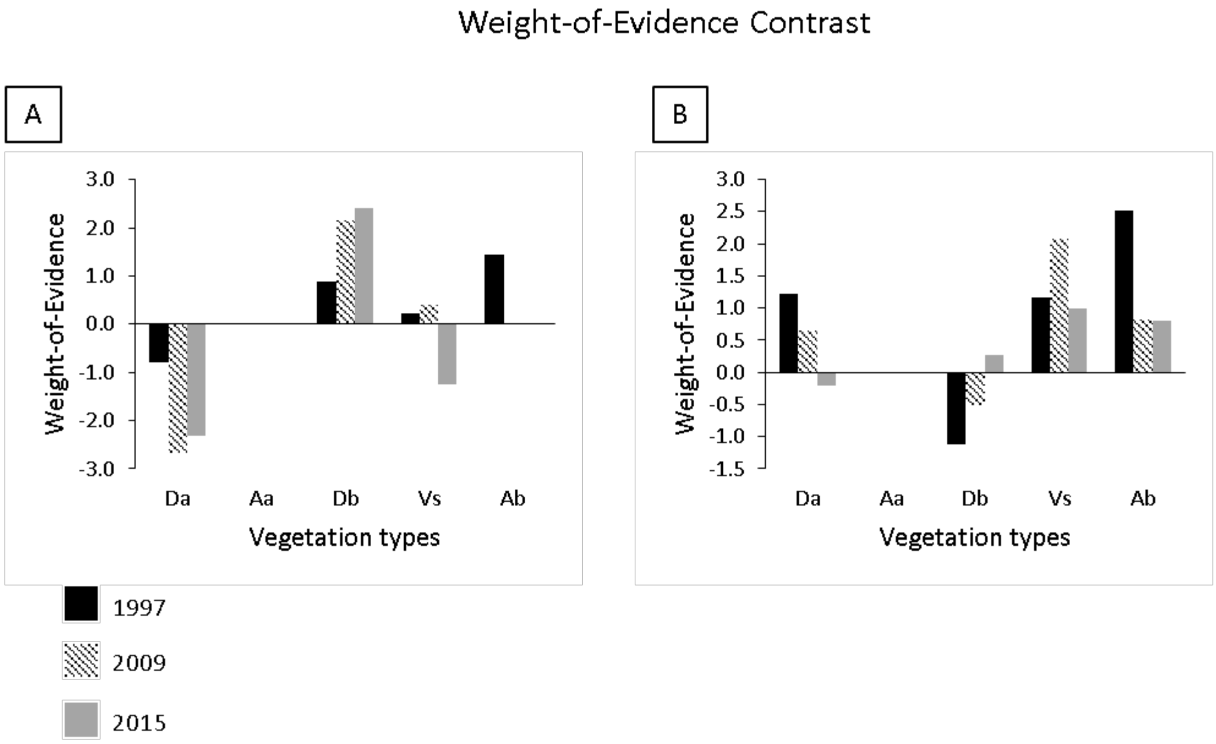

Figure S5: Values of weights-of-evidence contrasts for (A) Forest fire and (B) Deforestation for each vegetation type. Da = Dense-canopy rainforest on river floodplains; Aa = Open-canopy rainforest on river floodplains; Db = Dense-canopy rainforest on nonflooding lowlands; Vs = Secondary forests; Ab = Open-canopy rainforest on nonflooding lowlands.

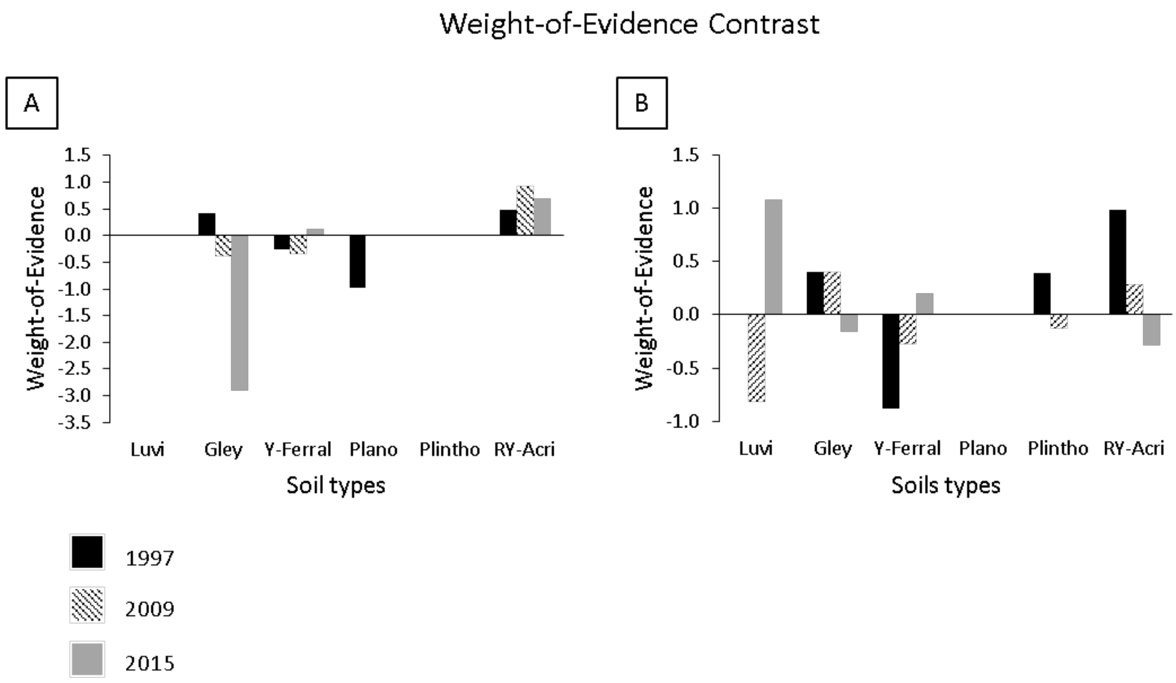

Figure S6: Values of weights-of-evidence contrasts for (A) Forest fire and (B) Deforestation for different soil types. Luvi = Luvisols; Gley = Gleysols; Y-Ferral = Yellow Ferrasols; Plano = Planosols; Plintho- Plinthosols; RY-Acri = Red Yellow Acrisol.

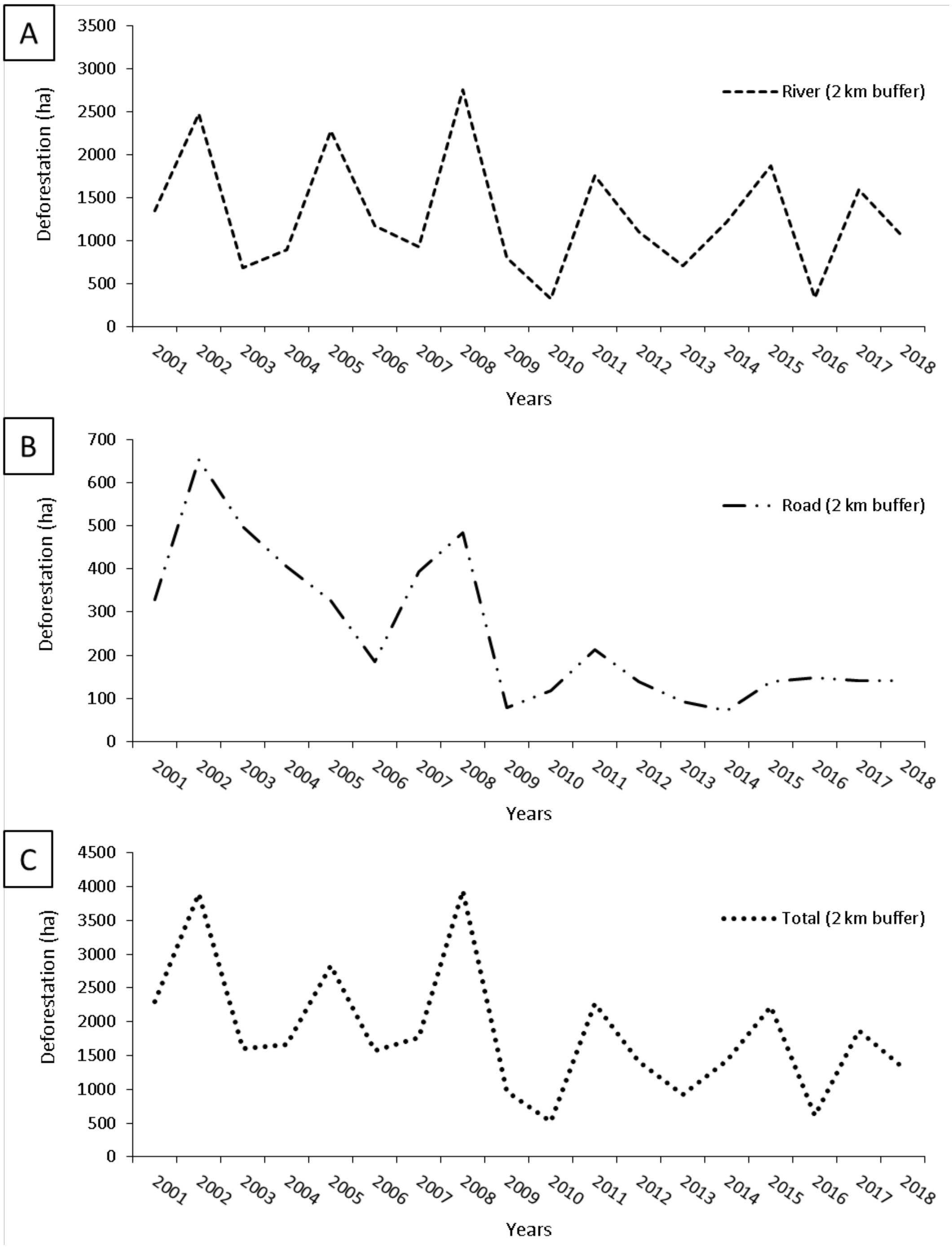

Figure S7: Deforestation from 2001 to 2018 within (A) a 2-km buffer from rivers, (B) a 2-km buffer from roads and (C) in the two buffers merged.